Liquid Crystals
Publication details, including instructions for authors and subscription information:
http://www.informaworld.com/smpp/title~content=t713926090

The peculiar optic, dielectric and X-ray diffraction properties of a fluorinated de Vries asymmetric diffuse cone-model ferroelectric liquid crystal

Jan P. F. Lagerwall[a]; David Coleman[b]; Eva Körblova[c]; Chris Jones[b]; Renfan Shao[b]; José M. Otón[d]; David M. Walba[c]; Noel Clark[b]; Frank Giesselmann[a]
[a] Institute of Physical Chemistry, University of Stuttgart, D-70569 Stuttgart, Germany [b] Department of Physics, Condensed Matter Laboratory, University of Colorado, Boulder, CO 80309 [c] Department of Chemistry and Biochemistry, University of Colorado, Boulder, CO 80309 [d] Dept Tecnología Fotónica, ETSI Telecomunicacin, Univ. Politécnica de Madrid, E-28040 Madrid, Spain

To cite this Article Lagerwall, Jan P. F. , Coleman, David , Körblova, Eva , Jones, Chris , Shao, Renfan , Otón, José M. , Walba, David M. , Clark, Noel and Giesselmann, Frank(2006) 'The peculiar optic, dielectric and X-ray diffraction properties of a fluorinated de Vries asymmetric diffuse cone-model ferroelectric liquid crystal', Liquid Crystals, 33: 1, 17 — 23
To link to this Article: DOI: 10.1080/02678290500454081
URL: http://dx.doi.org/10.1080/02678290500454081

Liquid Crystals, Vol. 33, No. 1, January 2006, 17–23

Taylor & Francis
Taylor & Francis Group

The peculiar optic, dielectric and X-ray diffraction properties of a fluorinated de Vries asymmetric diffuse cone-model ferroelectric liquid crystal

JAN P.F. LAGERWALL*†, DAVID COLEMAN‡, EVA KÖRBLOVA§, CHRIS JONES‡, RENFAN SHAO‡, JOSÉ M. OTÓN ¶, DAVID M. WALBA§, NOEL CLARK‡ and FRANK GIESSELMANN†

†Institute of Physical Chemistry, University of Stuttgart, Pfaffenwaldring 55, D-70569 Stuttgart, Germany
‡Department of Physics, Condensed Matter Laboratory, University of Colorado, Boulder, CO 80309, USA
§Department of Chemistry and Biochemistry, University of Colorado, Boulder, CO 80309, USA
¶Dept Tecnología Fotónica, ETSI Telecomunicacin, Univ. Politécnica de Madrid, E-28040 Madrid, Spain

(*Received 19 April 2005; accepted 2 September 2005*)

A new semi-fluorinated chiral smectic liquid crystal, W504, is investigated by electro-optic, dielectric and X-ray scattering experiments. It exhibits a huge dielectric soft mode response, strong electroclinic effect and a birefringence which increases considerably with the director tilt angle θ; typical characteristics of a SmA*–SmC* transition following the de Vries asymmetric diffuse cone (ADC) model in which the non-zero director tilt in SmC* arises through an ordering of tilting directions rather than an actual increase in average molecule tilt $\langle\theta_{mol}\rangle$. In W504 a small increase in $\langle\theta_{mol}\rangle$ of about 4° is however detected in the SmC* phase. Although the increase in molecule inclination is much less than the increase in director tilt θ, saturating close to 30°, it leads to a shrinkage of the smectic layers by about 1 Å, a result of the large initial molecule tilt in the SmA* phase, $\langle\theta_{mol}\rangle_{SmA*}\approx 30°$. The tilting transition in W504 is thus mainly an ADC model disorder–order transition, but it also has a component of a structural transition. The semi-fluorinated molecular structure of W504 leads to a very weak electron density modulation along the layer normal, giving a vanishing form factor in bulk samples which exhibit no (0 0 1) X-ray scattering peak. In thin films the (0 0 1) peak is however observed, indicating that the electron density modulation is enhanced by the breaking of the head–tail symmetry of the liquid crystal phase at the LC–air interface.

1. Introduction

In the research on ferroelectric and antiferroelectric liquid crystals (FLCs and AFLCs), i.e. materials exhibiting the chiral smectic C (SmC*) phase or one or more of its variants, considerable attention has over the last few years been directed towards compounds exhibiting the unusual property of a smectic layer thickness which is essentially independent of the director tilt angle θ [1–14]. In the SmC* phase the director **n** is inclined by an angle $\theta>0$ with respect to the smectic layer normal, **k**, a geometry which in combination with chirality results in a spontaneous polarization $\mathbf{P}_s$ along $\mathbf{n}\times\mathbf{k}$ [15]. Normally, the layers contract below the transition from the SmA* phase, where $\theta\equiv 0$ in the absence of fields, to the SmC* phase or one of its AFLC variants. In some compounds this shrinkage is much smaller than expected, a behaviour which was explained by the Dutch–American crystallographer Adriaan de Vries. He recognized that one must take into account that the molecules have a non-zero average inclination $\langle\theta_{mol}\rangle$ away from **k** even if $\theta=0$, as in SmA*, a result of the orientational disorder characteristic of any LC phase [16–19]. The uniaxial symmetry around **k** and the absence of director tilt are consequences of the fact that all directions of molecule inclination are equally probable in the orientational fluctuations.

In de Vries' scenario for the SmA–SmC transition without layer shrinkage, $\langle\theta_{mol}\rangle$ remains constant, while the increasing director tilt $\theta>0$ comes about through a gradual azimuthal biasing towards a certain molecule inclination direction. He referred to this model as the 'asymmetric diffuse cone' (ADC) model [19], the asymmetry being equivalent to the azimuthal biasing present in the SmC phase. The 'diffuse cone' can be seen as the trajectory over time of a single molecule fluctuating around **n** in any LC phase. Recent analysis of the ADC model has shown that, in the case of chiral smectics, it implies that the birefringence Δn strongly

*Corresponding author.
Email: jan.lagerwall@ipc.uni-stuttgart.de

Liquid Crystals
ISSN 0267-8292 print/ISSN 1366-5855 online © 2006 Taylor & Francis
http://www.tandf.co.uk/journals
DOI: 10.1080/02678290500454081

increases with θ [5] and that the SmA* electroclinic effect and soft mode (field-induced tilt $\theta>0$ and the corresponding polarization fluctuation) are unusually large [1, 20]. These properties have indeed been identified in a number of compounds with minimal layer shrinkage.

To date, ADC behaviour has been found mainly in mesogens that have at least one terminal chain quite different from standard alkyl chains, e.g. heavily fluorinated chains [2, 6–8, 10, 11, 13], with a siloxane moiety attached [4, 5, 9], or even with the mesogens attached to a polysiloxane backbone [12, 14]. In this paper we describe X-ray scattering, dielectric and electro-optic investigations of a new FLC (figure 1) of the former class, exhibiting several of the properties typical of ADC materials to a very strong degree, for instance a huge dielectric response. However, its X-ray scattering response is quite peculiar. Not only does the compound exhibit stronger layer shrinkage than most ADC materials investigated so far, but the first order X-ray scattering peak is essentially undetectable when studying bulk samples. The new results make it clear that the SmA*–SmC* transition can involve several mechanisms in parallel, and that even when the ADC model mechanism is strongly dominant it does not necessarily give temperature-independent smectic layer thickness.

2. Experimental

The liquid crystal compound W504 (synthesized in the Boulder chemistry lab) was filled into cells with three different types of alignment layers: standard commercial polyimide-coated EHC cells, hard-buffed polyimidecoated cells from the Chalmers MC2 cell production line (Gothenburg, Sweden) and nylon-coated cells made in the Madrid cleanroom. The cells were kept in Instec mK2 or Julabo FP-25 hot stages for temperature control. Sample texture observations and optic and electro-optic measurements were made using an Olympus BH-2 polarizing microscope. The optical tilt angle θ and birefringence Δn were measured with high resolution using a temperature scanning technique developed by Saipa and Giesselmann [21]. The magnitude of the spontaneous polarization $\mathbf{P}_s$ was measured by integrating the polarization reversal current while switching the sample with a triangular waveform electric field [22]. Dielectric spectroscopy with simultaneous sample texture monitoring was performed using an HP4192A impedance bridge, a USB video camera (Logitech) and DiScO measurement software (FLC Electronics).

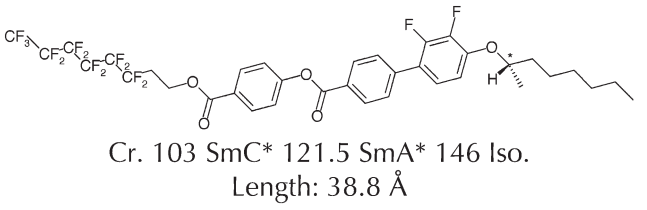

Figure 1. The molecule under investigation, (*S*)-W504. The length is the largest core–core distance resulting from conformational energy minimization with MOPAC/AM1, plus one F and one H van der Waals radius.

Three series of X-ray diffraction (XRD) experiments were carried out, in two locations. In the Stuttgart lab (Cu-K_α generator) the small angle scattering (SAXS) from unaligned samples in 0.7 mm diameter Mark capillary tubes was investigated with a Kratky compact camera and a 1D position sensitive detector (A. Paar); the wide angle scattering (WAXS) pattern from samples aligned by a 2.5 T magnetic field was determined using a flat film camera loaded with digital imaging plates (Fuji BAS-SR system). With the National Synchrotron Light Source at Brookhaven National Laboratory (beamline X10A) experiments were carried out in reflectivity mode on samples aligned homeotropically on an octadecyltriethoxysilane self-assembled monolayer (OTE SAM), as well as in transmission mode on capillary samples.

3. Results and discussion

3.1. *Textures and electro-optic behaviour*

Similar to other fluorinated ADC compounds [8] W504 is difficult to align in standard LC sample cells. Figure 2 shows representative textures in the SmA* and SmC* phases in the three different cell types used. Nylon has previously been shown to be one of the best alignment materials for this type of compounds [23] and, indeed, the nylon-coated cell produced excellent uniform alignment in the SmA* phase, figure 2 (*a*). As the sample was cooled into the SmC* phase, however, both domain types (corresponding to the two possible in-plane director tilt directions) developed a director structure with a strong twist from substrate to substrate. This led to poor maximum extinction and to washed-out colours, in bright orientations, changing with sample orientation and not reflecting the birefringence, cf. figures 2 (*b*) and 2 (*c*). Thus this cell was unsuitable for measurements of the optical properties of W504.

The SmC* twist was much less pronounced in cells coated with polyimide (PI) but the standard commercial cells (EHC, row 2 in figure 2) did not impose a uniform direction of the smectic layer normal, rendering quantitative measurements impossible also with this cell. However, it is qualitatively clear already from the colour change from yellow to orange on cooling the

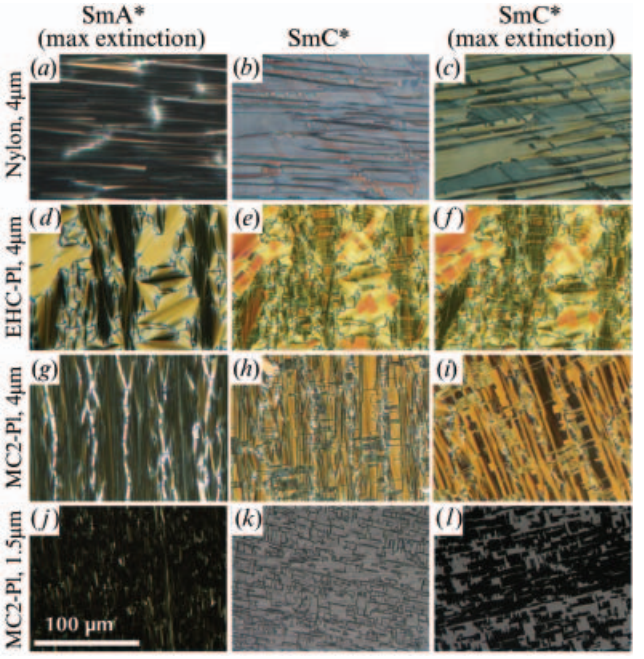

Figure 2. Textures of W504 in four different cells. In the left and right columns the sample has been aligned for maximum extinction (within some uniformly aligned region in *c*, *d*, *f*, *i* and *l*) in the SmA* and in the SmC* phase, respectively. The centre column shows the SmC* texture with the sample aligned as in the left column. The SmA* pictures are taken at $T=130^{\circ}$ and the SmC* pictures at $T=105^{\circ}$.

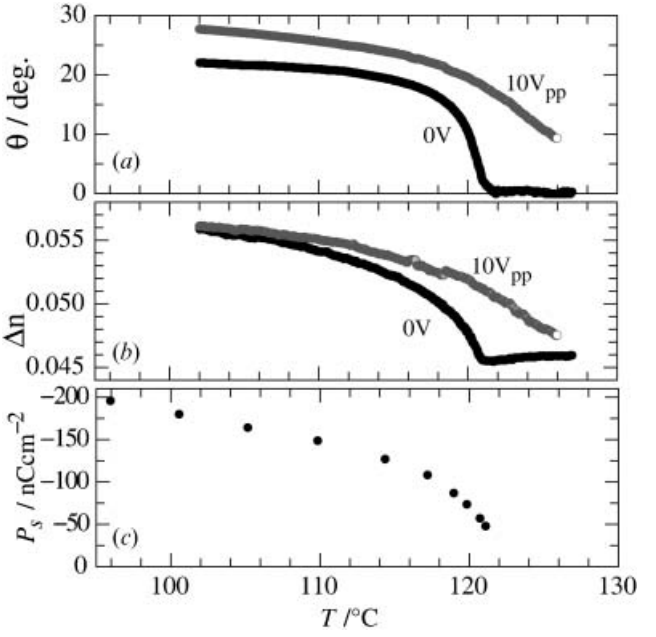

Figure 3. Optical director tilt angle θ (*a*), birefringence Δn (*b*) and spontaneous polarization $\mathbf{P}_s$ (*c*) as a function of temperature, the two former measured at 633 nm wavelength on a 1.5 μm cell in the absence of field and with an applied electric field ensuring saturated switching.

4 μm sample from SmA* (*d*) to non-helical SmC* (*e* and *f*), that Δn increases substantially in the SmC* phase, as expected for ADC materials. In the (partially) helical regions the colour remained yellow, a result of the helical averaging of the optic axis direction decreasing the effective value of Δn. The yellow–orange colours also reveal that Δn is lower than in most smectic compounds, which in a 4 μm cell typically exhibit colours between red and blue, i.e. at the border between first and second order in the Michel–Levy interference colour chart.

By using strongly buffed PI cells, we achieved a sufficiently homogeneous alignment and at the same time avoided the director twist in SmC*, as shown in the two lowest rows in figure 2. Decreasing the cell gap to 1.5 μm, a relatively defect-free alignment was obtained (*j–l*), allowing quantitative measurements of Δn and θ. The thin cell gap also assured complete helix and twist expulsion even in the absence of fields, allowing for measurements also in the field-free state. The results are shown in figures 3 (*a*) and 3 (*b*). In addition to the remarkably low values of birefringence, the typical ADC characteristic of Δn increasing with θ stand out from these measurement results. The birefringence at the low temperature limit of the SmC* phase (the first measurements were taken in supercooled SmC*) is about 22% larger than in field-free SmA*. As is also typical of ADC materials, the magnitude of the electroclinic effect is very large, with an induced tilt of $\theta \approx 10^{\circ}$ about 5°C above the SmA*–SmC* transition, and a corresponding field-induced increase of Δn. Both the θ and the Δn curves are continuous, with no discrete jump around the SmA*–SmC* phase transition, which thus seems to be of second order. Indeed, DSC measurements at 10 K min^{-1} heating and cooling rates could not resolve any transition peak, confirming the continuous nature of the transition.

3.2. *Spontaneous polarization and dielectric response*

The value of the spontaneous polarization, $\mathbf{P}_s$, is shown as a function of temperature in figure 3(*c*). It has a negative sign and reaches the quite substantial value of -200 nC cm^{-2} (in supercooled SmC*). Considering the high magnitude of $\mathbf{P}_s$ a quite strong dielectric response should be expected, but the actual dielectric spectra that we obtained on a 23.5 μm planar-aligned (PI coating) sample by far surpassed all expectations. At minimum measuring field strength, the dielectric loss ε'' reached values above 500 in the SmC* phase, figure 4(*a*), where the response can be attributed to a phason mode corresponding to helix distortion. This was however only about half of the maximum response, which was

detected at the SmA*–SmC* transition and can thus be attributed to the soft mode. Such behaviour is unheard of in normal FLCs, where the SmC* phason mode is usually much stronger than the soft mode, but it was recently shown to be a characteristic of chiral ADC compounds [20]. The strong soft mode is a result of the very weak restoring force counteracting director tilt (and, consequently, polarization) fluctuations in the ADC mechanism. This peculiarity follows from the fact that the director tilt in SmC* arises mainly through an azimuthal tilt direction ordering. With ε'' almost reaching 1000 at the SmA*–SmC* transition, the soft mode response of W504 is by far the strongest known to us, being even more than twice as strong as that of the ADC compound from 3M studied in [20]. This difference scales quite well with the difference in the θ–$\mathbf{P}_s$ coupling constant, being two to three times smaller in the 3M compound than in W504.

On increasing the field strength to $20\,\mathrm{mV\,\mu m^{-1}}$ — a quite typical field strength for low amplitude dielectric spectroscopy investigations on FLCs — the phason mode absorption grew drastically in strength, raising ε'' in the SmC* phase to values around 1 600, thereby overshadowing the soft mode response at the phase transition, cf. figure 4(*b*). This very strong SmC* response arises because the measuring field induces not only helix distortion, but even the start of helix unwinding. This was verified by studying the texture photomicrographs taken during the measurement, two examples of which are shown in the insets of figures 4(*a*) and 4(*b*). The periodic helix lines were easy to see in the pictures taken during the $2\,\mathrm{mV\,\mu m^{-1}}$ scans, but were partially or completely absent during the scans with $20\,\mathrm{mV\,\mu m^{-1}}$ measuring field strength. Such a low helix unwinding/switching threshold is very unusual among FLCs but it has been reported also for other ADC compounds, even in the case of AFLCs [7].

In order to make it clear just how large the dielectric response of W504 is, an absorption spectrum of (*S*)-S1B8, a typical non-ADC FLC with similar $\mathbf{P}_s$ (saturating at $-160\,\mathrm{nC\,cm^{-2}}$) is shown in figure 4 (*c*) (see Schacht *et al.* [24] for more details on this compound). The measurement was performed in the same type of cell, with the same thickness, at 2 and $20\,\mathrm{mV\,\mu m^{-1}}$, giving essentially identical spectra. The data are plotted with the same scaling as in figures 4 (*a*) and 4 (*b*). The phason and soft mode absorptions of S1B8, producing ε'' values of about 50, are then hardly visible. (Actually, the main absorption seen in figure 4 (*c*), at low frequencies of 10–100 Hz, is not due to the polar nature of the SmC* phase but to a relatively large conductivity of the sample.)

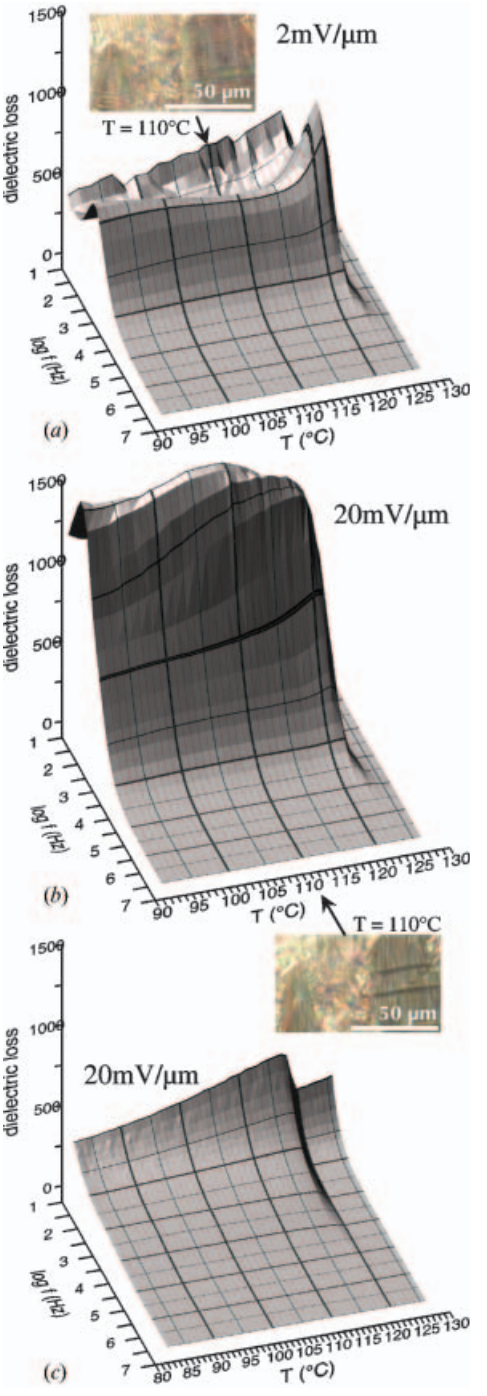

Figure 4. Dielectric absorption spectra from W504 in a 23.5 μm planar-aligned cell (*a* and *b*) at two amplitudes of the measuring field. $20\,\mathrm{mV\,\mu m^{-1}}$ is enough to unwind the helix in the SmC* phase, as seen in the two examples of texture photomicrographs taken during the measurement. The helix unwinding leads to the large increase in SmC* absorption in (*b*). As comparison, the corresponding dielectric spectrum of (*S*)-S1B8, an ordinary non-ADC FLC with $\mathbf{P}_s$ similar to that of W504, is shown (*c*) with the same axis scalings as for W504. The SmA*–C* transition is at 119° in S1B8, at 121.5° in W504.

3.3. *X-ray scattering results*

We studied the XRD profiles of W504 both in the small angle and in the wide angle regimes. Examples of SmA* and SmC* radial SAXS profiles are shown in figures 5(*a*) and 5(*b*) as a function of scattering vector magnitude q. During the measurements with Cu-K_α radiation (*a*) we noted that the scattering intensity was generally very weak (exposure times 2–5 times longer than usual were used). The biggest surprise however was that no (0 0 1) pseudo-Bragg peak corresponding to the smectic layering could be resolved at any temperature above crystallization in the expected range of $q \sim 0.18$ (equivalent to a layer thickness of $\sim$35 Å). In the SmA* phase a diffuse increase in intensity could be seen at about twice this scattering angle (which would correspond to the (0 0 2) peak) but this 'bump' was too small to be reliably analysed. The very unusual absence of first order smectic XRD peak suggests that the form factor is close to zero, a characteristic which most likely is related to the electron-rich fluorinated end chain of W504. Although only one chain is fluorinated, the head–tail symmetry in a bulk LC sample results in equal numbers of molecules where this chain points mainly upwards or downwards. Hence the effective electron density can be quite similar in core and tail regions. The unusually weak modulation in electron density along the layer normal could thus explain the vanishing form factor.

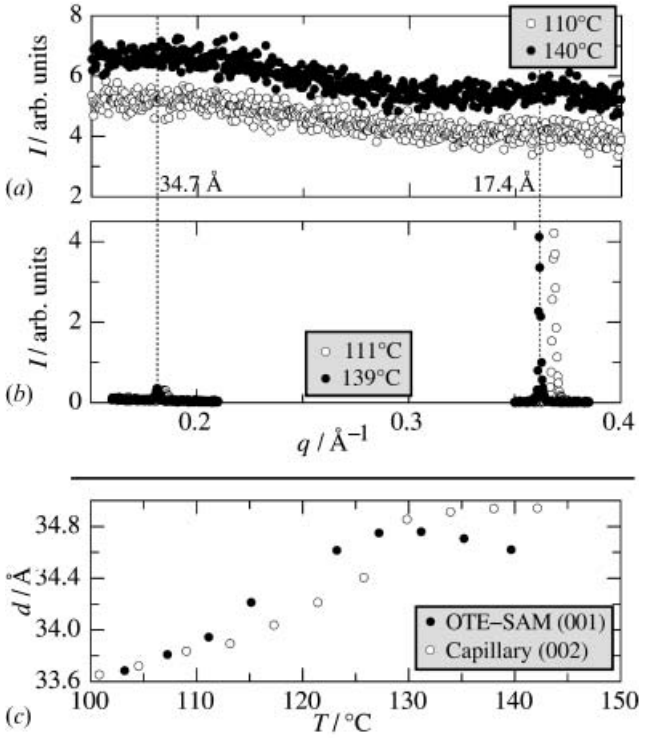

Figure 5. Small-angle X-ray scattering profiles from a non-aligned sample investigated with Cu-K_α radiation (*a*) and from an OTE-SAM-aligned sample investigated at the synchrotron source (*b*), of W504 in the SmA* (140/139°) and SmC* (110/111°) phases. From the synchrotron data the smectic layer spacing d as a function of temperature T was extracted (*c*).

With the well aligned OTE-SAM sample investigated at the synchrotron source, diffraction profiles where the smectic layer peaks are easy to resolve could however be obtained, even though the intensity of the (0 0 1) peak was still much lower than that of (0 0 2), cf. figure 5(*b*). We speculate that the scattering in the case of the OTE-SAM sample is enhanced by the breaking of the head–tail symmetry at the LC–SAM and LC–air interfaces. Close to the sample surface we may expect a large difference in the numbers of molecules aligned fluorine tail up or down. As it is the near-surface volume of the sample that contributes to the reflectivity measurement, this experiment would then sense a larger electron density contrast than during the experiment on bulk samples. Hence the form factor is non-zero, rendering the (0 0 1) peak visible.

In contrast, when repeating the bulk LC measurements on capillaries at the synchrotron, no (0 0 1) peak was visible but a weak (0 0 2) peak was observed, just as with the Kratky camera measurements. In figure 5(*c*) we present the smectic layer spacing d vs. temperature obtained from the capillary and OTE samples. While there appears to be a slight shift in the transition temperatures and in the d-spacing, the data are qualitatively equivalent, indicating that the scattering peak observed in capillary samples is indeed the (0 0 2) peak of the smectic layering, and that the form factor is approximately zero at the (0 0 1) peak. The issue of the varying scattering behaviour of W504 in different sample geometries is currently being investigated more thoroughly and will be reported in a future paper.

We note that the smectic layer spacing in SmA*, $\sim$35 Å, corresponds to an average tilt of the molecular long axis with respect to the layer normal, $\langle\theta_{\mathrm{mol}}\rangle$, of about 26° (using the molecule length obtained with MOPAC/AM1, cf. figure 1). Such a large average molecule tilt in the SmA* phase is typical for ADC compounds [8, 9], whereas in ordinary materials it is 15–20° [18]. On the other hand, the smectic layers in W504 exhibit a non-negligible contraction below the SmA*–SmC* transition which is somewhat of a surprise considering the very strong ADC characteristics observed in the electro-optic and dielectric response. To understand this we need to investigate the temperature variation of $\langle\theta_{\mathrm{mol}}\rangle$. The best way to assess $\langle\theta_{\mathrm{mol}}\rangle$

is to analyse the directional (azimuthal) distribution of the wide angle X-ray scattering—originating from the liquid-like intralayer molecular order—in the SmA* and SmC* phases.

The non-polar and uniaxial orientational order in, for example, a nematic or smectic A liquid crystal is described by the orientational distribution function (ODF) $f(\beta)$ where β denotes the angle between the long molecular axis and the director of the uniaxially ordered phase. Since **n** is co-linear with **k** in SmA/SmA*, $\beta \equiv \theta_{\mathrm{mol}}$ in this phase. The ODF is usually expanded in terms of Legendre polynomials with the expansion coefficients $\langle P_2 \rangle$, $\langle P_4 \rangle$,... defining the orientational order parameters S_2, S_4, etc. Experimentally, we can determine $f(\beta)$ and the related order parameters in the SmA* phase by analysing the azimuthal intensity profile $I(\chi)$ in the WAXS pattern. The angle χ indicates the scattering direction and we define it such that the magnetic field is directed along $\chi = \pm 90^\circ$. Since **n** in SmA* aligns with the field, this is also the direction of **k**.

For our analysis, we use a procedure developed by Davidson, *et al.* [25] where the ODF is expanded in terms of $\cos^{2n}\beta$-functions:

$$f(\beta) = \sum_{n=0}^{\infty} f_{2n} \cos^{2n} \beta. \qquad (1)$$

The corresponding WAXS intensity profile can also be written as a series of $\cos^{2n}\chi$ functions involving the same f_{2n},

$$I(\chi) = \sum_{n=0}^{\infty} f_{2n} \frac{2^n n!}{(2n+1)!!} \cos^{2n} \chi. \qquad (2)$$

Hence, by fitting equation (2) to the experimental scattering profile $I(\chi)$, with the f_{2n} being the parameters to fit, $f(\beta)$ can be directly calculated by inserting the fitted f_{2n} into the expansion in equation (1). With $f(\beta)$ known, any average $\langle X \rangle$ of a certain property X that is related to the orientational distribution can be numerically calculated, e.g. S_2, and $\langle \theta_{\mathrm{mol}} \rangle$. In the SmC* phase, however, the WAXS pattern includes the orientational averaging due to the helical superstructure, hence S_2 cannot be extracted (being uniaxially symmetric, the Legendre polynomial order parameters are not defined in the biaxial SmC* phase).

In figure 6 the WAXS intensities measured in SmA* and SmC* are plotted as a function of χ, together with the corresponding best fits of equation (2). The resulting values of $\langle \theta_{\mathrm{mol}} \rangle$ and S_2 are also given. We note that the orientational order determined in the SmA* phase is remarkably low, $S_2 = 0.52$, corresponding to $\langle \theta_{\mathrm{mol}} \rangle_{\mathrm{SmA^*}} \approx 33^\circ$. This is a characteristic that W504 shares with previously investigated

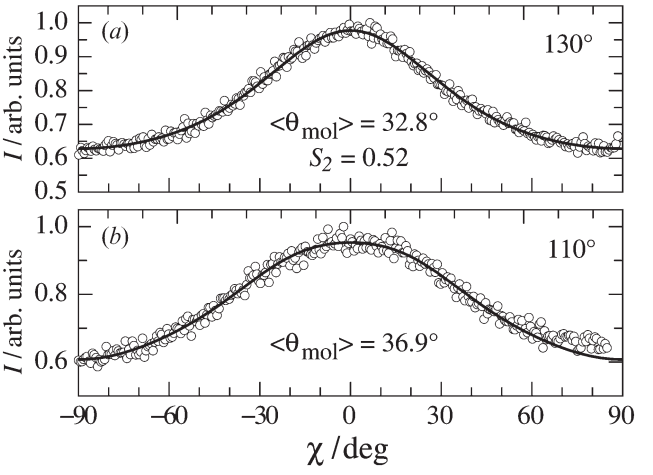

Figure 6. WAXS scattering profile (rings) in the SmA* (*a*) and SmC* (*b*) phases, the corresponding best fits of equation (2) (black curve) and the resulting average molecular inclination with respect to the smectic layer normal $\langle \theta_{\mathrm{mol}} \rangle$. For the SmA* phase the orientational order parameter S_2 can also be estimated.

ADC materials [8, 9]. However, the value obtained with this method estimates S_2 downwards, i.e. the real (local) orientational order may be sligthly higher, and $\langle \theta_{\mathrm{mol}} \rangle$ slightly smaller. This is because our measurement averages the order over a macroscopic volume, hence phenomena such as layer undulations and sample mosaicity contribute negatively to the measured value of S_2. However, the low Δn values, and the fact that the smectic layer spacing in SmA* is much smaller than the expected molecule length, suggest that the local orientational order indeed is low in W504.

On cooling the sample to the SmC* phase, the WAXS profile broadens somewhat, reflecting a small increase of average molecule inclination, at 110°C being close to 37°. This constitutes an important difference to the ADC material investigated in [8], where d was largely unaffected by the SmA*–SmC* transition and where the WAXS patterns in SmA* and SmC* could hardly be distinguished. Although the broadening in W504 is small, corresponding to an increase of $\langle \theta_{\mathrm{mol}} \rangle$ of only about 4°, the large starting value of the molecular tilt angle gives the increase a considerable impact on d, about 5% shrinkage. (Had $\langle \theta_{\mathrm{mol}} \rangle_{\mathrm{SmA^*}}$ been zero, the tilt increase would have had to be 18° to produce such shrinkage.) Taking d in SmA* to be about 35 Å the WAXS analysis would thus predict a shrinkage of 1.8 Å, which is more than the actual shrinkage. This is another indication that the influence of layer undulations and sample mosaicity on the WAXS pattern produce apparent $\langle \theta_{\mathrm{mol}} \rangle$ values which are too large. The relative

increase of about 4° should however be close to the real $\langle\theta_{mol}\rangle$ increase. The much larger increase in the optical tilt angle θ displayed in figure 3 is thus due to the strong ADC aspect of the SmA*–SmC* transition in W504, i.e. it can be attributed mainly to an ordering of tilting directions, in accordance with the electro-optic and dielectric behaviour of the compound.

4. Conclusions

The non-zero director tilt in the SmC* phase of the semi-fluorinated mesogen W504 can be largely attributed to an ordering of tilting directions of molecules which exhibit a considerable tilt already in the SmA* phase. This compound is thus quite well described by the asymmetric diffuse cone (ADC) model of de Vries, as verified by a birefringence Δn which increases strongly with director tilt θ, strong electroclinic effect and huge dielectric soft mode response in the SmA* phase, and a wide angle X-ray diffraction pattern which changes relatively little between SmA* and SmC*. However, in contrast to a number of other ADC smectics which have recently been investigated, there is a non-negligible layer shrinkage of about 1 Å below the SmA*–SmC* transition in W504. This is a result of the large starting magnitude of the average molecule tilt with respect to the smectic layer normal in the SmA* phase, $\langle\theta_{mol}\rangle_{SmA^*} \approx 30^\circ$, giving even the small increase of about 4° detected on cooling W504 into SmC* a considerable impact on the layer spacing. Counter-intuitively, through the large average molecule tilt in SmA*, the ADC aspect thus increases the sensitivity of the layer spacing to changes in molecule tilt. While a negligible layer shrinkage is still a strong indication of ADC behaviour, we conclude that it is not a requirement.

X-ray scattering profiles from bulk samples of W504 contain no (0 0 1) X-ray scattering peak. This highly unusual feature can be understood by considering that the combination of one fluorinated chain and one ordinary alkoxy chain, taking the head–tail symmetry of the bulk liquid crystal phase into account, leads to a very weak electron density modulation along the smectic layer normal, and thus a vanishing form factor. The head–tail symmetry is however broken at the liquid crystal–air and liquid crystal–substrate interfaces, hence a thin film of W504 on an OTE-SAM substrate, examined in reflection, exhibits a non-zero form factor. Consequently, a (0 0 1) scattering peak is then observed in the scattering profile, allowing for the determination of the smectic layer spacing.

Acknowledgments

J.L. gratefully acknowledges financial support from the Alexander von Humboldt Foundation and from the Swedish Research Council.

References

[1] F. Giesselmann, P. Zugenmaier, I. Dierking, S.T. Lagerwall, B. Stebler, M. Kaspar, V. Hamplova, M. Glogarova. *Phys. Rev. E.*, **60**, 598 (1999).
[2] M.D. Radcliffe, M.L. Brostrom, K.A. Epstein, A.G. Rappaport, B.N. Thomas, R.F. Shao, N.A. Clark. *Liq. Cryst.*, **26**, 789 (1999).
[3] Y.P. Panarin, V. Panov, O. Kalinovskaya, J.K. Vij. *J. mater. Chem.*, **9**, 2967 (1999).
[4] M.S. Spector, P.A. Heiney, J. Naciri, B.T. Weslowski, D.B. Holt, R. Shashidhar. *Phys. Rev. E.*, **61**, 1579 (2000).
[5] J.V. Selinger, P.J. Collings, R. Shashidhar. *Phys. Rev. E.*, **64**, 061705 (2001).
[6] N.A. Clark, T. Bellini, R. Shao, D. Coleman, S. Bardon, D.R. Link, J.E. Maclennan, X.H. Chen, M.D. Wand, D.M. Walba. Walba, *et al. Appl. Phys. Lett.*, **80**, 4097 (2002).
[7] F. Giesselmann, J.P.F. Lagerwall, G. Andersson, M.D. Radcliffe. *Phys. Rev. E.*, **66**, 051704 (2002).
[8] J.P.F. Lagerwall, F. Giesselmann, M.D. Radcliffe. *Phys. Rev. E.*, **66**, 031703 (2002).
[9] P. Collings, B. Ratna, R. Shashidhar. *Phys. Rev. E.*, **67**, 021705 (2003).
[10] S.T. Wang, X.F. Han, Z.Q. Liu, A. Cady, M.D. Radcliffe, C.C. Huang. *Phys. Rev. E.*, **68**, 060702R (2003).
[11] J.P.F. Lagerwall, F. Giesselmann, A. Saipa, R. Dabrowski. *Liq. Cryst.*, **31**, 1175 (2004).
[12] M. Rössle, R. Zentel, J. Lagerwall, F. Giesselmann. *Liq. Cryst.*, **31**, 883 (2004).
[13] C. Huang, S. Wang, X. Han, A. Cady, R. Pindak, W. Caliebe, K. Ema, K. Takekoshi, H. Yao. *Phys. Rev. E.*, **69**, 041702 (2004).
[14] M. Rössle, L. Braun, D. Schollmeyer, R. Zentel, J.P.F. Lagerwall, F. Giesselmann, R. Stannarius. *Liq. Cryst.*, **32**, 533 (2005).
[15] R.B. Meyer, L. Liebert, L. Strzelecki, P. Keller. *J. Phys. Lett.*, **36**, L69 (1975).
[16] A. de Vries. *J. chem. Phys.*, **71**, 25 (1979).
[17] A. de Vries. *Mol. Cryst. liq. Cryst. Lett.*, **49**, 179 (1979).
[18] A. de Vries, A. Ekachai, N. Spielberg. *Mol. Cryst. liq. Cryst. Lett.*, **49**, 143 (1979).
[19] A. de Vries. in *Advances in Liquid Crystal Research and Applications*, L. Bata (Ed.), pp. 71–80, Pergamon Press, Oxford, Budapest (1980).
[20] M. Krueger, F. Giesselmann. *Phys. Rev. E.*, **71**, 041704 (2005).
[21] A. Saipa, F. Giesselmann. *Liq. Cryst.*, **29**, 347 (2002).
[22] K. Miyasato, S. Abe, H. Takezoe, A. Fukuda. *Jpn. J. appl. Phys. Lett.*, **22**, L661 (1983).
[23] M. Radcliffe. personal communication (2002).
[24] J. Schacht, H. Baethge, F. Giesselmann, P. Zugenmaier. *J. mater. Chem.*, **8**, 603 (1998).
[25] P. Davidson, D. Petermann, A.M. Levelut. *J. Phys. (Paris) II*, **5**, 113 (1995).